The Hanle Effect

1   Introduction

The object of this experiment is to measure the intensity (related to the polarization state) of the fluorescent light from a sample cell containing mercury vapor, as a function of the applied magnetic field. From this data, you will determine the lifetime of the $^3P_1$ excited state of mercury. [*Please read pages 1–8 of the Zeeman Effect writeup for additional review of magnetic moments and angular momentum addition.*]

Unlike many of the experiments conducted in this modern physics lab, Hanle's explanation of his 1924 experiment (that demonstrated the variation of polarization of the resonance fluorescent light in a weak magnetic field) was not well accepted at first. For that matter, Hanle was not even the first to observe this phenomenon. It was actually reported first by Wood in 1912; and in 1922, R.W. Wood and A. Ellett published a paper describing the effect of a magnetic field on the polarization of resonance fluorescence radiation. It turned out that for the 253.7 nm light from Hg absorption cell, magnetic fields of a few gauss were sufficient to depolarize the resonance fluorescence light. Wood and Ellett soon realized that this behavior could not be interpreted as a Zeeman effect since the Zeeman separation in such fields is very small compared to typical Doppler-broadened linewidths of such radiation. Hanle's real credit comes for his classical explanation of the effect. However, typical of the criticism of his interpretation is the statement made by the distinguished physicist Max Planck who said to Hanle, "your interpretation cannot be correct, it contradicts quantum theory." Of course, modern quantum mechanics was not yet born and most theorists were convinced that his effect was a kind of Faraday effect (see below).

1.1   The Faraday Effect

It is known that the Faraday effect yields a rotation of the plane of polarization in a magnetic field when light travels through a dispersive medium. The Faraday rotation has the same sense as the Larmor precession associated with the Zeeman effect in both the right and left wings of the finite-width absorption line, but the rotation sense is reversed for frequencies close to the center of the absorption line. For the Hanle effect, only the central part of the line is active and the observed rotation of the polarization is always in the *same* sense as the precessional motion. Furthermore, the Faraday effect causes the rotation to be proportional to the length of the path in the medium within the magnetic field. For the Hanle effect, the rotation effect reaches its maximum as soon as the sample experiences the longitudinal magnetic field and there is absolutely *no* dependence on the length of the path traveled by the exciting light in the magnetic field, nor on the path traveled by the fluorescence light in the magnetic field before detection.

In conclusion, the Hanle effect is not a form of the Faraday rotation!

1.2   Level Crossing Spectroscopy

It is said that the Hanle effect is a type of level crossing experiment. If energy levels are split in an external magnetic field, then in the range from weak to medium-strength fields, the levels can indeed cross. Such crossings occur when there is already a fine-structure splitting in the absence of a magnetic field B_0, or when there are hyperfine multiplets with the same **J** angular momentum.

Let us consider two possible resonance transitions, generically labeled as "g" in Fig. 1, from excited states b and c, each of which could be populated by the absorption of a photon labeled as "f" transitioning from the ground state a. Both transitions could be excited simultaneously by
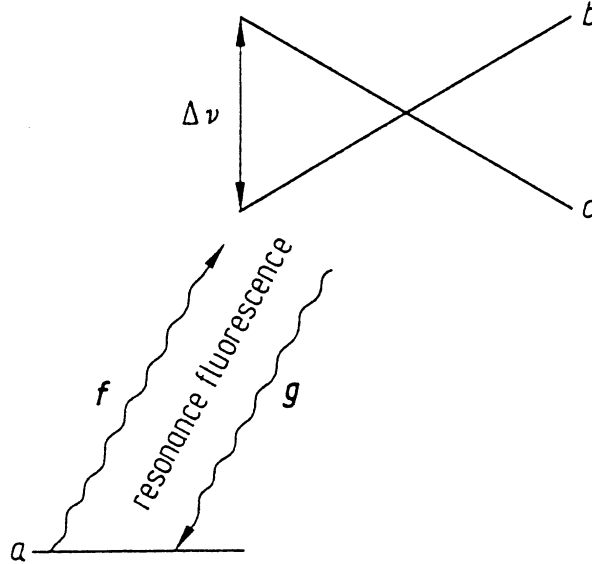

Figure 1: Generic energy level diagram with two crossed excited states. Photons labeled as "f" can be absorbed from state a to these two states, b and c, because, even when they are not crossed, the quantity $\Delta\nu$ is smaller than the typical Doppler-broadened light source. The photons labeled as "g" are in the fluorescence light that can be detected.

the Doppler-broadened resonance light from some light source. Each excited state could return separately to the ground, where the sum of the individual intensities is observed by some photo-detector. If we assume, for example, that each state b or c by itself emits a linearly polarized wave with amplitudes $A_b \cos(\omega_b t)$ or $A_c \cos(\omega_c t)$ respectively, then the total intensity of the observed resonance light (when there is no level crossing) is proportional to $A_b^2 + A_c^2$, on the average.

Now, assume that the two levels cross. The transition frequencies are then the same. Both levels are coherently excited, and the light waves emitted from them can interfere. Thus, the observed intensity is now proportional to $(A_b + A_c)^2$. In this case, there is a change in the spatial distribution of the emitted radiation (in analogy to double-slit interference), and in the direction of observation, one generally sees a change in the observable total intensity whenever the external B-field produces a crossing of two such levels. Furthermore, if linearly polarized light is used for the excitation light, it is possible to excite coherently two magnetic sublevels with the same transition frequency (in fact, share the same photon), if the selection rule for the one is $\Delta m = +1$, while the selection rule for the other is $\Delta m = -1$. Both are fulfilled by the linearly polarized light which can be decomposed into a σ^+ and a σ^- photon. The σ^- components excites the $\Delta m = -1$ transition, and the σ^+ component excites the $\Delta m = +1$ transition.

The significance of this method is that it yields very high spectral resolution. The precision with which the crossing field can be measured (the so-called linewidth in this level-crossing spectroscopy) is **not** limited by the Doppler width of the spectral lines because here the coherence of the excitation within an individual atom is being utilized. In this case, the linewidth becomes limited by the lifetime of the excited state.
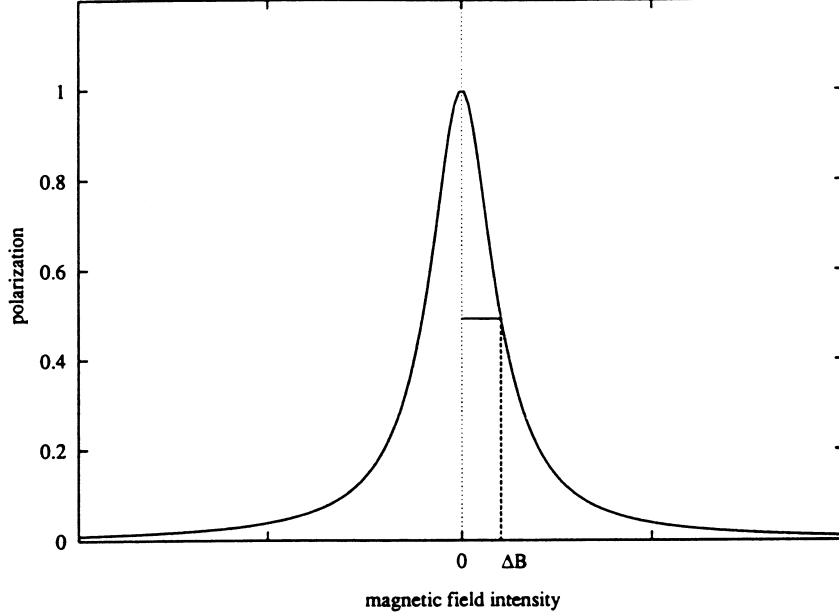
Figure 2: The degree of polarization of fluorescence light is plotted as a function of magnetic field.

In a similar manner, the *Hanle effect* can be thought of as a zero-field, level crossing experiment. Configuration terms which are <u>not</u> split without the aid of an applied B-field "cross" in zero field, when B_0 is varied from negative values to positive values and vice versa. In zero field, degenerate atoms may be coherently excited for the same reasoning as in the level-crossing spectroscopy, assuming the validity of the selection rules.

1.3   Observation of Polarization

An example of the changes in the degree of polarization of fluorescence light from an absorption cell versus B_0-field is shown in Fig. 2. The quantity ΔB in the figure represents the half-field width where the polarization is half its maximum value at $B_0 = 0$. To better understand this figure, one must first investigate some of the possible orientations of $\vec{B}_0$ where it is assumed that the incident light travels along the $\hat{z}$-direction and the observer looks at the fluorescence radiation along the $\hat{y}$-direction; see Fig. 3 through Fig. 8. For the given directions given in these figures, the polarization degree is defined as

$$P = \frac{I_x - I_z}{I_x + I_z} \tag{1}$$

where I_x and I_z are the intensities of the x- and z-linearly polarized components of the output fluorescence light. The expected experimental observations are as follows:

- Case-1: There is no change in polarization for any value of B_x [see Fig. 3].

- Case-2: There is no change in polarization for values of the magnetic field at the extremes, $B_z = 0$ and B_z very large [see Fig. 4].
  The intensity will decrease to half as B_z becomes large.

- Case-3: When $B_y = 0$, the linear polarization is seen to be in the $\hat{x}$-direction [see Fig. 5].
  When $B_y \neq 0$, but small, there is decreased polarization, slightly tilted from the $\hat{x}$-direction

3

(i.e. E'_z is small, but in phase with E'_x).

When $B_y \neq 0$, but large, strongly unpolarized light is observed (i.e. random phase angle between E'_x and E'_z comes from the ensemble of atoms).

- Case-4: When $B_x = 0$, no light intensity is observed [see Fig. 6].
  When $B_x \neq 0$, but small, a weak intensity with polarization in the $\hat{z}$-direction is observed.
  When $B_x \neq 0$, but large, a strong intensity with polarization in the $\hat{z}$-direction is observed.

- Case-5: When $B_z = 0$, no light intensity is observed [see Fig. 7].
  When $B_z \neq 0$, but small, a weak intensity with polarization in the $\hat{x}$-direction is observed.
  When $B_z \neq 0$, but large, a strong intensity with polarization in the $\hat{x}$-direction is observed.

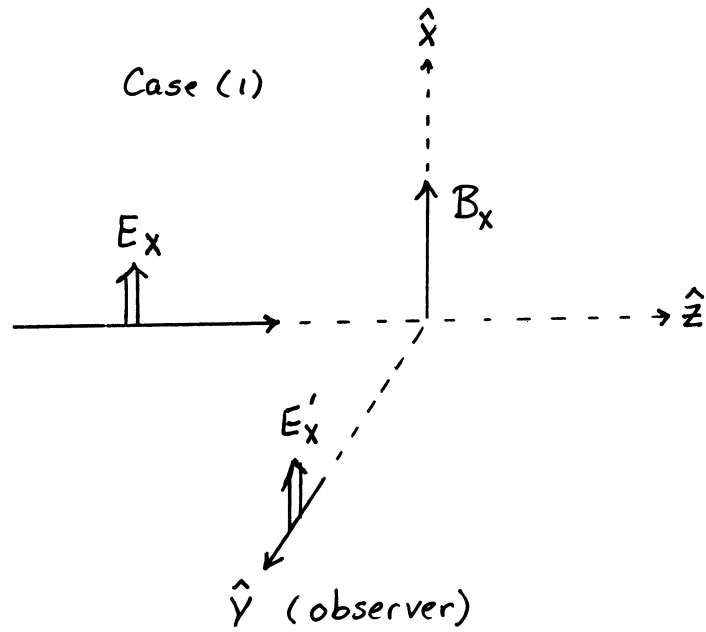- Case-6: No light is seen for any value of B_y [see Fig. 8].

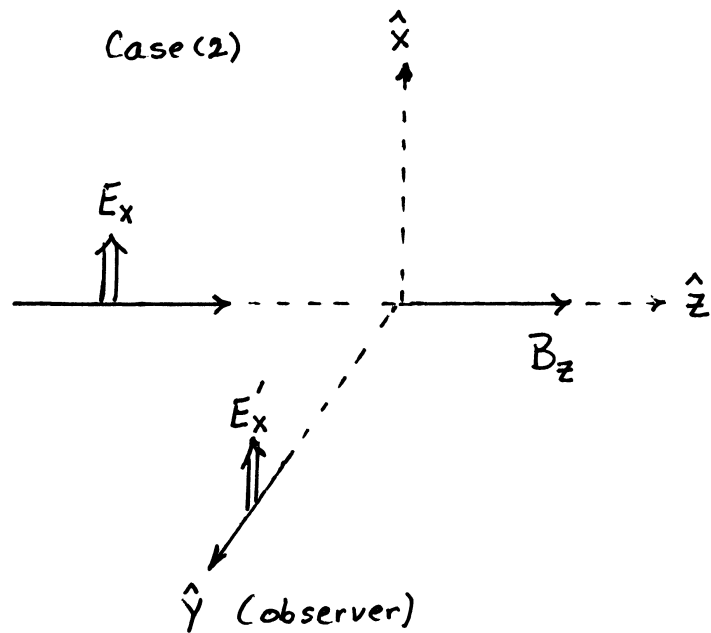Figure 3: Initial polarization is in the $\hat{x}$-direction and $\vec{B}$ is along the same direction

Figure 4: Initial polarization is in the $\hat{x}$-direction and $\vec{B}$ is along the $\hat{z}$-direction.
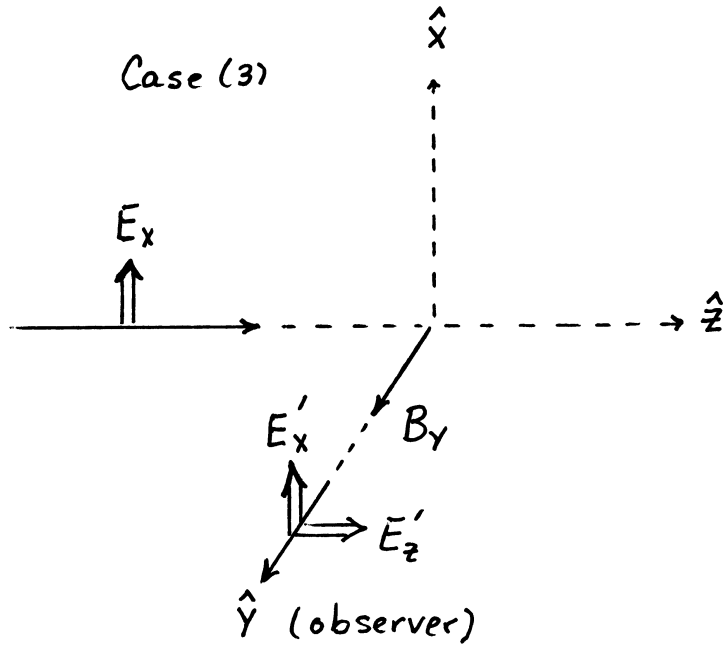
Case (3)

$\hat{x}$

E_x

$\hat{z}$

E'_x B_Y

$\bar{E}'_z$

$\hat{Y}$ (observer)

Figure 5: Initial polarization is in the $\hat{x}$-direction and $\vec{B}$ is along the $\hat{y}$-direction.

Case (4)

$\hat{x}$

B_X

$\hat{z}$

E_Y

E'_z

$\hat{y}$ (observer)
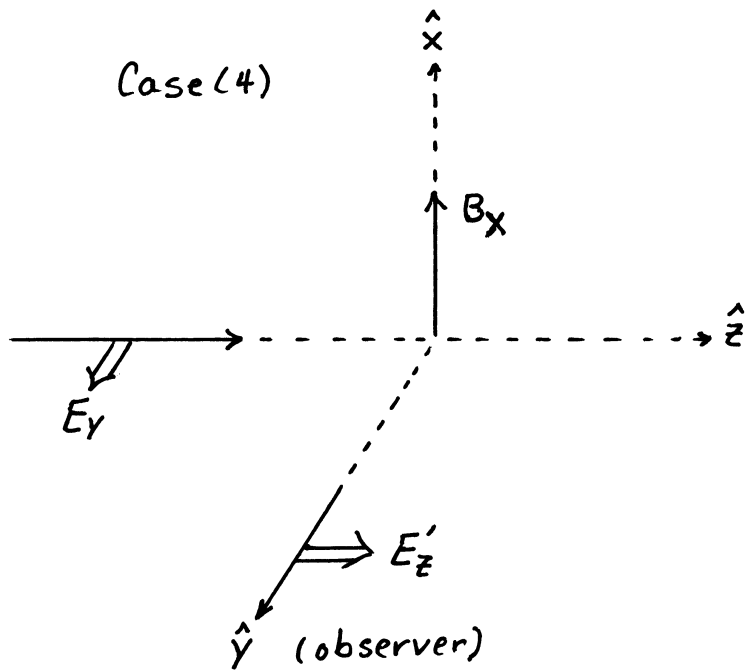
Figure 6: Initial polarization is in the $\hat{y}$-direction and $\vec{B}$ is along the $\hat{x}$-direction.

Case (5)

$\hat{x}$

$\hat{z}$

$B_{\hat{z}}$

E_Y

E'_x

$\hat{y}$ (observer)
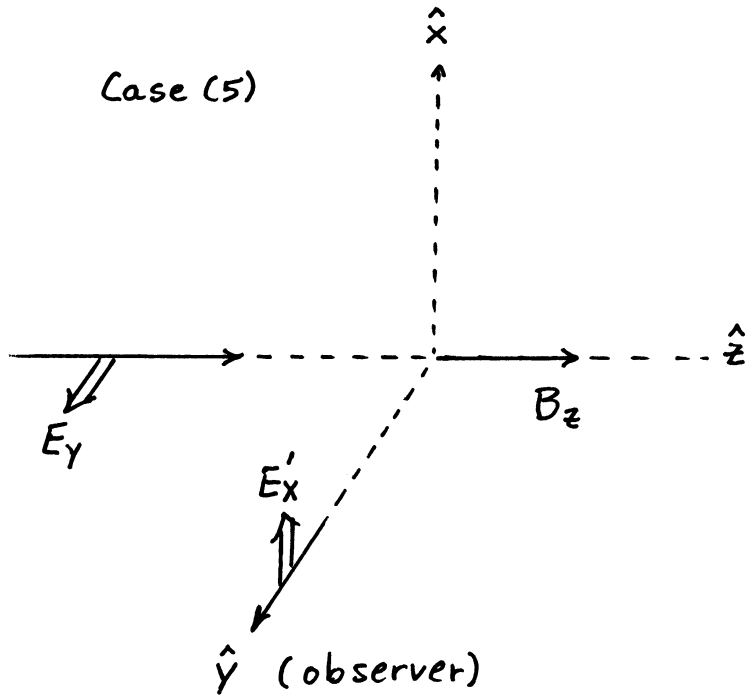
Figure 7: Initial polarization is in the $\hat{y}$-direction and $\vec{B}$ is along the $\hat{z}$-direction.

Case (6)

$\hat{x}$
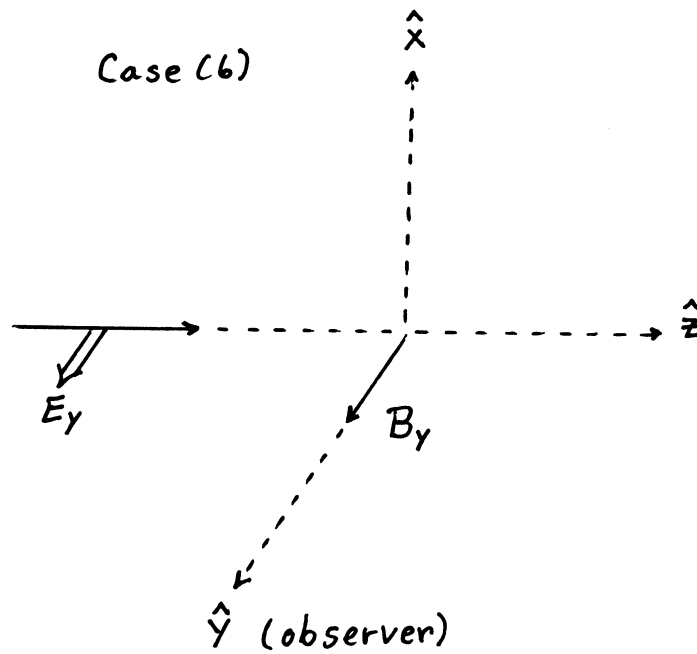
$\hat{z}$

E_Y

B_Y

$\hat{y}$ (observer)

Figure 8: Initial polarization is in the $\hat{y}$-direction and $\vec{B}$ is along the same direction.

1.4 Classical Description of the Effect

It is possible for classical theory to explain all the results described in Sec. 3, if one considers the optically-active electron in mercury to act as a classical oscillator that is set in motion parallel to the direction of the polarization of the exciting light. The radiation emitted by the oscillator will be polarized in the same direction as the incident light, thus explaining the results observed along the $\hat{y}$-axis when the incident beam is polarized parallel to the $\hat{x}$-direction and $B = 0$. Incidentally, one should also remember that a classical oscillator can not radiate in the direction of its vibration. Thus, when the incident light is polarized parallel to the $\hat{y}$-direction, classical theory says that no light can be seen along the y-axis, when $B = 0$.

The experiments with various orientations of nonzero B-fields are also explained by classical theory when one remembers that the electron's magnetic moment will precess about a magnetic field, giving rise to circularly polarized light when viewed along the field and yielding linearly-polarized light when viewed perpendicular to the field (i.e. the classical Zeeman effect). Figure 9 illustrates a plausible arrangement of B-field causing the precession of the orbital magnetic moment, $\vec{\mu}_L$, as the momentum $\vec{P}$ from the electric dipole oscillation is carried around the path of the precession along with $\vec{\mu}_L$. Since $\vec{P}$ does not convey any angular momentum, it does <u>not</u> require additional energy
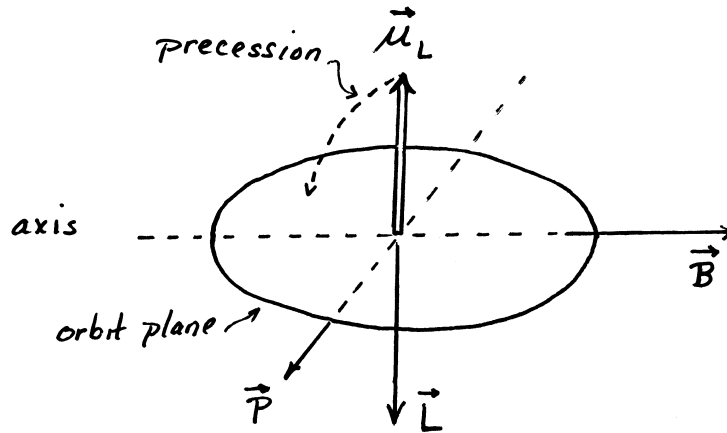

Figure 9: Plausible illustration of how the electric dipole momentum is made to precess around the magnetic field direction.

to rotate it in space. Thus, when the electric vector of the exciting light is in the $\hat{x}$-direction, and there is a strong magnetic field parallel to the $\hat{z}$-axis [i.e. Case (2)], the electron of the classical model will precess about the $\hat{z}$-axis and light intensity observed along the $\hat{y}$-direction (i.e. along the initial direction of $\vec{L}$ in Fig. 9) will be reduced by a factor of two. This case leaves the polarization still along the $\hat{x}$-axis, since the simple harmonic components (in the $\hat{y}$-direction) of the circular rotation can not be seen.

In order to explain arrangements like that shown in Case (3) in which the light becomes depolarized with increasing field, we need only invoke the classical model of a damped oscillator. In Case (3), the oscillator begins vibrating in the $\hat{x}$-direction, but will precess about the field, all the while its amplitude of vibration is dying down with time. If viewed along the direction of the field, the path that the oscillator takes is in the form of a rosette pattern. If the angular precession velocity is large compared to the damping rate, the rosette will be symmetrical as shown in the upper half of Fig. 10. Here, this constraint means B is large or effectively $\omega_L \gg 1/\tau$ where τ is the
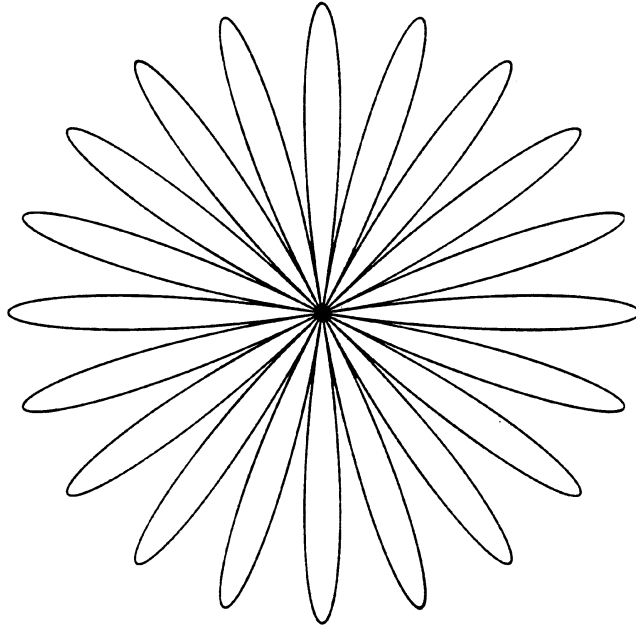
The rosette motion of an undamped charged oscillator in a magnetic field.
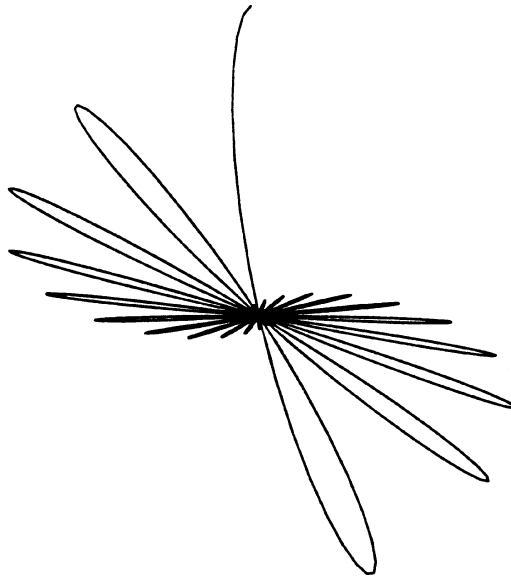
The damped rosette motion obtained by taking radiative decay into account.

Figure 10: The time-configurations for the classical oscillator that precesses around the magnetic field for the undamped (upper half) and the damped (lower half) cases. These form symmetrical and un-symmetrical rosette patterns respectively.

mean-damping time and $\omega_L = g_J(\mu_B/\hbar)B$ is the Larmor frequency for magnetic moment $\vec{\mu_J}$ and $\mu_B = e\hbar/2m_e$ is the the Bohr magneton. Thus, for a perfectly symmetrical rosette, the observed radiation from an ensemble of such oscillators will show unpolarized light, being that each such oscillator randomly damps in all 2π of phase. However, if the damping rate is comparable to ω_L, the form is an incomplete rosette, as shown in the lower half of Fig. 10. The resulting radiation will be partially polarized (i.e. less than when $B = 0$), with its direction of polarization rotated relative to the vertical $\hat{x}$-axis.

1.5   Classical Intensity Calculation

Now imagine Case (4) when the direction of the classical electron oscillator has rotated through an angle ϕ relative to the $\hat{y}$-direction of observation at time $t = 0$. Then, the amount of intensity observed dI in an observation interval dt is proportional to $[\sin^2 \phi]e^{-t/\tau}dt$ where $\sin^2 \phi$ comes from the dipole radiation pattern as usual and $e^{-t/\tau}dt$ represents the dipoles available to radiate between t and $t + dt$. Thus, for continual excitation and observation,

$$I = C \int_0^\infty \left[1 - \cos(2\omega_L t)\right]e^{-t/\tau}dt \tag{2}$$

where $\phi = \omega_L t$ and $2\sin^2 \phi = 1 - \cos(2\phi)$, with constant C yet to be determined. Upon completing the integration, one finds

$$I = \frac{C\tau}{2}\left[1 - \frac{1}{1 + (2\omega_L \tau)^2}\right]. \tag{3}$$

Now evaluating this result for large magnetic fields, one obtains $I_\infty = C\tau/2$, where I_0 is obviously zero as required for $B = 0$. Of special interest is the case when $I = I_\infty/2$, for which $B = \Delta B_{1/2}$. Here, one can show that $2\omega_L \Delta(B_{1/2}) = \pm 1$ and

$$\frac{1}{\tau} = 2g_J \frac{\mu_B}{\hbar}|\Delta B_{1/2}| \tag{4}$$

As shown in Fig. 11, the value of $\Delta B_{1/2}$ occurs when the intensity changes from half its value between I_{min} and I_{max}. This quantity can be used to determine the lifetime of the excited state. For your experiment, you could use unpolarized light incident onto the absorption cell since, from Case (1), the component E_x does not get affected by B_x. This component merely adds a constant field-independent background to your signal shown in Fig. 11. You should note that one could also use Case (5) in this experiment, for which $\vec{B}$ is along the $\hat{z}$-direction. However, one could not use unpolarized light to measure τ, as you should be able to deduce from this model.

1.6   Quantum-Mechanical Treatment

It should be clear by now that there must be a rigorous quantum mechanical explanation for the existence of this zero-field level-crossing spectroscopy which we call the Hanle effect. The following will only briefly outline the treatment, since there are several good accounts in the literature, such as the one in the article entitled "Measurement of Atomic Lifetimes by the Hanle Effect" by R. deZafra and W. Kirk, Amer. J. Phys. **35**, 573 (1967). In this article, the authors point out that the easiest point of departure from classical physics is in the use of the Breit equation [G. Breit,
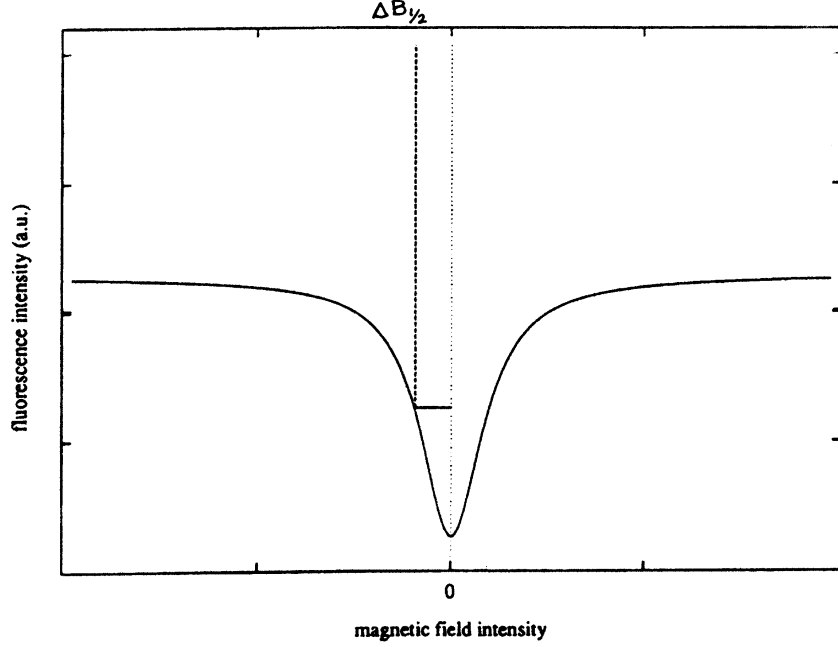
Figure 11: Observed intensity versus swept net-magnetic field. The dip to a minimum in intensity occurs at $B_{net} = 0$ and $\Delta B_{1/2}$ is the half-width at half height between I_{max} and I_{min}. The signal does not always go to zero at $B_{net} = 0$ because of such things as scattered uv-light and incomplete linear polarization.

Rev. Mod. Phys. **5**, 91 (1933)]:

$$R(f, g) = C \sum_{\mu\mu', mm'} \frac{f_{\mu m} f_{m\mu'} g_{\mu'm'} g_{m'\mu}}{1 - i(E_\mu - E_{\mu'})\tau/\hbar} \tag{5}$$

which represents the rate at which light of polarization $\vec{f}$ is absorbed and light of polarization $\vec{g}$ is re-emitted by a free atom (see Fig. 1). Here, C is a constant that is dependent on vapor-lamp intensity, absorber-atom density, geometrical factors, etc. The magnetic quantum numbers m and m' refer to the Zeeman sublevels of the ground state and μ and μ' refer similarly to sublevels of the excited state. Also, the quantity E_μ is the energy of the μ-th excited substate. Finally, the dipole transition-matrix elements between the substates in question, $f_{\mu m}$ and $g_{\mu m}$, are given by

$$f_{\mu m} = \langle \mu | \vec{f} \cdot \vec{r} | m \rangle \tag{6}$$
$$g_{\mu m} = \langle \mu | \vec{g} \cdot \vec{r} | m \rangle \tag{7}$$

where $\vec{r}$ is displacement vector along the dipole axis. Now, we generalize the $\vec{f}$ and $\vec{g}$ polarizations as in Fig. 12, where the incoming radiation, directed along the $\hat{z}$-axis, has polarization vector $\vec{f}$ making angle θ_1 relative to the $\hat{y}$-axis, and outgoing radiation, directed along the $\hat{y}$-axis, has polarization vector $\vec{g}$ making angle θ_2 relative to the $\hat{z}$-axis.

For $J = 0 \leftrightarrow J = 1$ ($^1S_0 \leftrightarrow^3 P_1$), the Breit equation reduces to

$$R(f, g) \propto R(\Delta\mu = 0) + R(\Delta\mu = 1) + R(\Delta\mu = 2) \tag{8}$$

where $\Delta\mu$ is the integer difference in excited-state magnetic quantum numbers, and

$$R(\Delta\mu = 0) = \frac{1}{2}[\cos^2\theta_1 \cos^2\theta_2 + \sin^2\theta_1 \sin^2\theta_2] \tag{9}$$
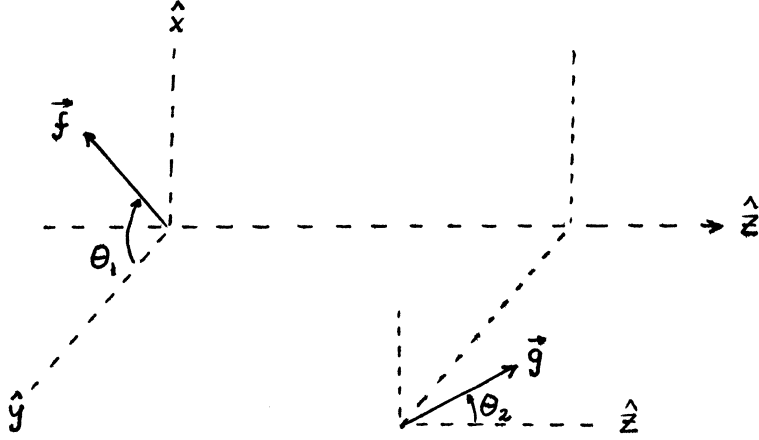
11

Figure 12: The arrangement of incoming polarization $\vec{f}$ and outgoing polarization $\vec{g}$ relative to the coordinate axes.

$$R(\Delta\mu = 1) = \cos\theta_1 \cos\theta_2 \sin\theta_1 \sin\theta_2 \left\{ \frac{2\Delta E\tau/\hbar}{1 + (\Delta E\tau/\hbar)^2} \right\} \tag{10}$$

$$R(\Delta\mu = 2) = -\frac{1}{2} \frac{\cos^2\theta_1 \cos^2\theta_2}{1 + (2\Delta E\tau/\hbar)^2} . \tag{11}$$

If one imposes the condition of *no* polarization on either the incoming or outgoing radiation, one must let θ_1 and θ_2 vary over all possible values, yielding $(\cos^2\theta_n)_{ave} = (sin^2\theta_n)_{ave} = 1/2$ while $(\cos\theta_n \sin\theta_n)_{ave} = 0$. Thus, we obtain the rate (which is related to the intensity of the fluorescence radiation)

$$R(f, g) = \frac{C'}{4} \left\{ 1 - \frac{0.5}{1 + (2\Delta E\tau/\hbar)^2} \right\}, \tag{12}$$

i.e. Cases (1) and (4) combined. However, for the case in which the input radiation is plane polarized in the yz-plane and no polarization analysis is made of the outgoing radiation, one finds

$$R(f, g) = \frac{C'}{4} \left\{ 1 - \frac{1}{1 + (2\Delta E\tau/\hbar)^2} \right\} \tag{13}$$

which corresponds exclusively to Case (4) and is given classically in Eq. (3) with $\hbar\omega_L = \Delta E$.

One should also note the following salient features of this treatment, as applied to our experiment. The $\Delta\mu = 0$ term contributes only a constant (magnetic-field-independent) term to the rate. The $\Delta\mu = 1$ term vanishes on the average, and the entire field-dependent effect comes from the $\Delta\mu = 2$ term. With our experimental geometry, mercury atoms are excited into a coherent superposition of the two eigenstates of the atomic Hamiltonian with $\mu = +1$ and $\mu = -1$. *If the separation between these levels is small compared to $\hbar/\tau$, i.e. if their energies overlap within their natural widths, coherent effects will be observed in the emitted fluorescence radiation.* And if we sweep the B-field from negative to positive values, we observe the bell-shaped Lorentzian curve shown in Fig. 11 for the intensity of the emitted radiation.
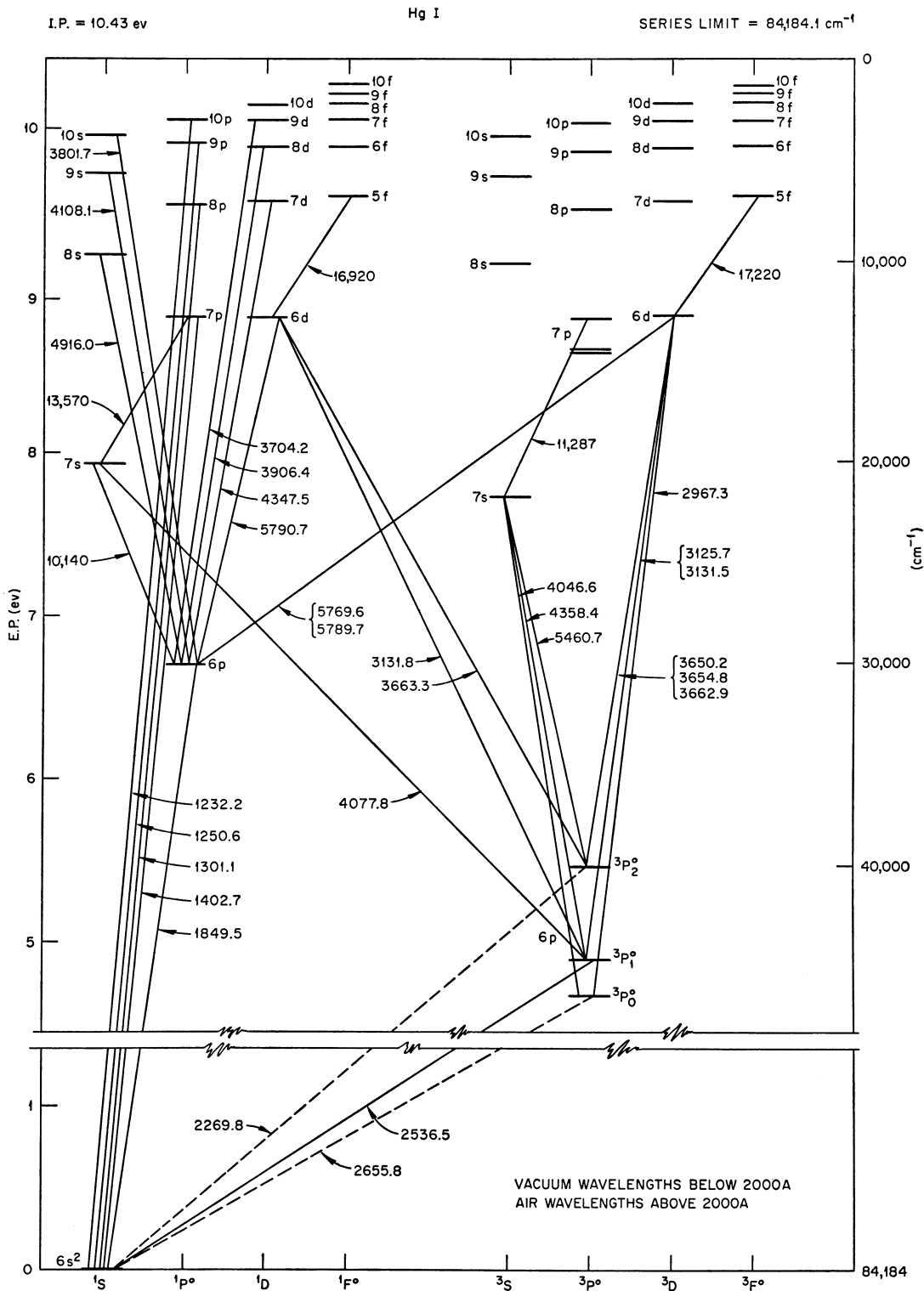
Figure 13: Grotrian diagram for the energy levels of the neutral mercury atom.

2   The Mercury Experiment

2.1   The Apparatus

In order to see the Hanle effect, our experiment will use the element mercury for the vapor in the absorption cell. Mercury (with a $^1S_0$ ground state) has the experimental advantage of a substantial vapor pressure at room temperature. In addition, good mercury vapor lamps for the production of resonance radiation are readily available. One disadvantage which Hg possesses is that its strongest resonance line, $^1S_0 \leftrightarrow^1 P_1$, is in the far ultraviolet at 185 nm (see Fig. 13) where even the best optical glass components fail.   Fortunately, the first forbidden inter-combination transition, $^1S_0 \leftrightarrow^3 P_1$, is a reasonably strong line owing to generous configuration mixing in mercury, and although this line is still in the uv at 253.7 nm, it provides no exceptional difficulties as long as special quartz optics are used throughout.

Figure 14 sketches a basic experimental setup which we could use for observing the Hanle effect. For our arrangement, though, the $\hat{y}$-axis is vertical and does <u>not</u> include a polarizer-2 since we do not wish to analyze the degree of polarization of the fluorescence radiation. There is, however, a special liquid-cell optical filter in the location that polarizer-2 would occupy, which filters out the visible radiation and passes uv-light, in order to make the photo-detector more sensitive to the wavelength of interest.

The orientation of the magnetic field in our experiment is also different from that shown in Fig. 14, where we have chosen $\vec{B}$ to be along the $\hat{x}$-direction and Case (4) is the one of interest. If polarizer-
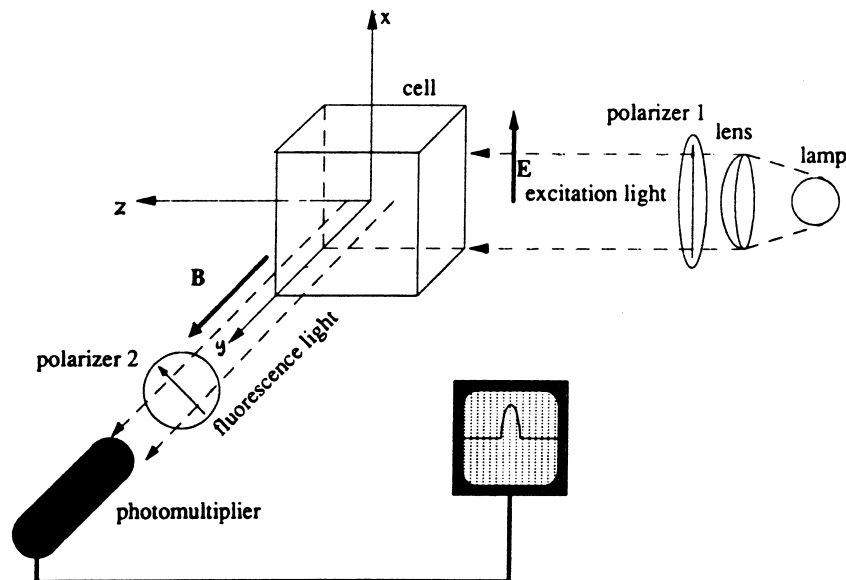
Figure 14: Basic setup for observing a Hanle-effect signal. The sample is contained in an absorption cell and is excited by appropriately polarized light into a superposition of quantum states. The polarization and intensity of the fluorescence light emitted along the B-field direction can be detected by a suitable photo-detector.

1, which is in the incident-light path, is rotated into the horizontal direction (i.e. along the $\hat{x}$-axis, then, there is no change in polarization or intensity of the fluorescence radiation since the B-field is parallel to the classical electron oscillation in this case and momentum $\vec{P}$ of Fig. 9 can not precess

around B_x. Thus, polarizer-1 must be in the vertical direction and should be adjusted to minimize the background light signal **when** $B_{\text{net}} = 0$. Failure to properly align the polarizer will yield a slight asymmetry in the line shape of the I-versus-B plot, with respect to reflection about $B_{\text{net}} = 0$. Since the transition lifetime is fairly long for mercury, the magnetic field variation which is required to produce the Hanle effect signal is quite small (i.e. $\Delta B_{1/2} \sim 0.5$ Gauss). Thus, some care must be taken to buck out the stray magnetic field in the lab which is dominated by the earth's relatively constant magnetic field.

The absorption cell must be made of quartz glass since our uv-light will not penetrate normal pyrex glass. The shape of our cell is that of a right-cylinder with flat quartz windows on each end. However, proper absorption cells should have the characteristic shape of a "Woods horn" type of scattering cell, as shown in Fig. 15. The purpose of the curved taper is to prevent internal backscattering of the incident light beam (which is therefore not fluorescence radiation). Hence, the proper shape will reduce the field-independent background light that is picked up by the photo-detector. Also, our cell contains a small drop of purified mercury, but the sample has not been isotope separated. This means that it contains both odd and even nuclear isotopes of Hg with natural abundances of 16.8% for ^{199}Hg, 13.2% for ^{201}Hg, and the remainder being even isotopes with nuclear spin $I = 0$. This fact led to one of the main sticking points in the early theoretical development of the Hanle effect which required 100% degree of polarization at zero field. However, only 90% was observed in those early cells. This was later found to be due to the appearance of hyperfine structure in the odd ($I \neq 0$) isotopes which must be taken into account in the proper quantum mechanical treatment.

2.2 Determining the excited-state lifetime

Since the object of this experiment is to determine the lifetime of the 6^3P_1 excited state in Hg, we must also address the issue of "coherent radiation trapping" of the fluorescence radiation. This effect is often referred to as "coherence narrowing" and is one of the major phenomena which can affect
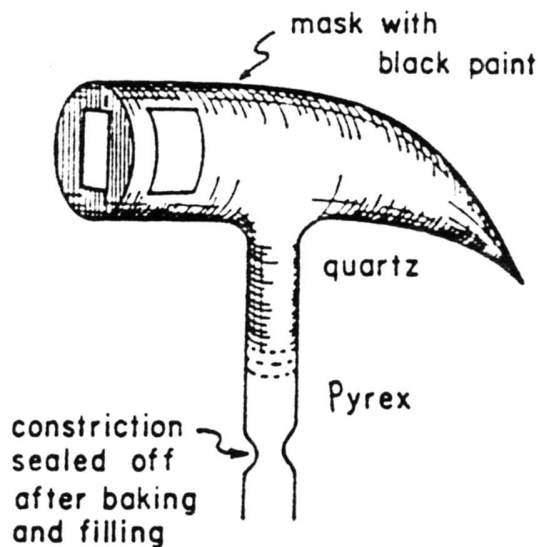

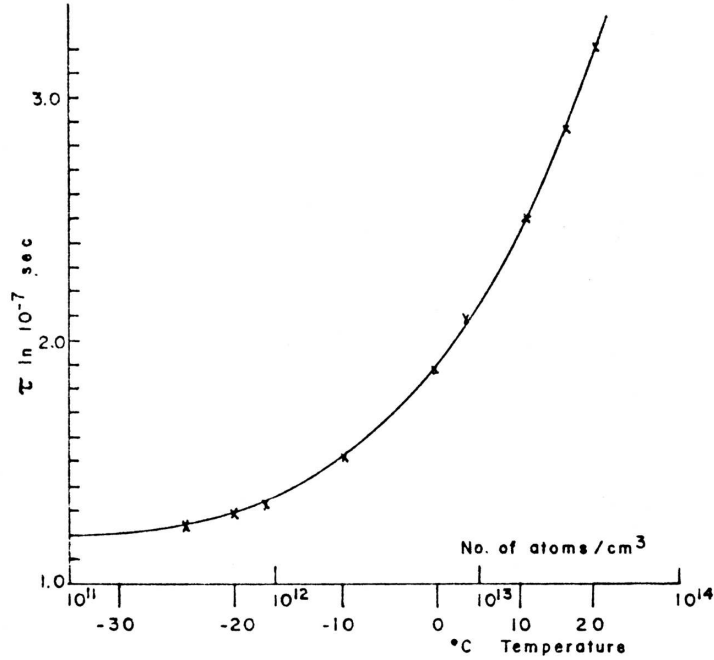Figure 15: Basic design for a "Wood's horn" type of light-absorption cell.

Figure 16: The effect of coherence narrowing on lifetimes measured at various densities of mercury vapor. The magnitude of the variation of τ with density depends on the size and design of the vapor cell. In other words, it is not a true density effect, but rather depends on the number of absorbing atoms along the line of observation.

Hanle-effect measurements, such as those made in Hg. This effect results when fluorescence light radiated by the decay of one atom is absorbed by another atom in a coherent fashion, preserving both the phase and orientation of the electric dipole vibration of the first atom. The newly excited atom then begins to precess in the B-field in phase with the original atom's precession, just as if the original excited atomic state lived longer (or equivalently had a narrower energy width). If the vapor is dense enough, and the absorption cross-sections are fairly large, this process may occur several times before the radiation finally escapes from the vapor, with an apparent lifetime being equal to the sum of the individual lifetimes for each coherent absorption.

One way to minimize this effect is to construct the entrance and exit windows very near to each other (but still at right angles). The entrance window in Fig. 15 would then be placed much closer to the exit wall in order to minimize the thickness of the slice of vapor through which the fluorescence radiation must pass. Another way to address this problem is to vary the vapor density and extrapolate to 0 K. An example of this scheme is shown in Fig. 16 [from data by M.W. Zemansky, Phys. Rev. **29**, 513 (1927)]. As you can see, room-temperature Hg-vapor might show a lifetime $\tau \sim 3 \times 10^{-7}$ sec, but this is not necessarily the value you will determine at your single measurement temperature of $\sim 20°$C. The reason is that coherence narrowing depends so critically on the size and shape of your particular absorption cell. For your information, Fig. 17 shows two tables of lifetimes measured using the Hanle effect; the lower table lists several measurements for the lifetime of the 6^3P_1 exited state of Hg.

16

Atom	Series notation of resonance line	Wave-length	τ in secs.	f-value	Author, reference and method
Mg	$3\,^1S_0-3\,^3P_1$	4571	$\sim4\times10^{-3}$	—	Frayne [9], § 7b
Zn	$4\,^1S_0-4\,^3P_1$	3076	$\sim1\times10^{-5}$	—	Soleillet, chap. v
,,	,,	,,	$\sim1\times10^{-5}$	—	Soleillet [71], § 3e
,,	$4\,^1S_0-4\,^1P_1$	2139	$<10^{-7}$	—	Soleillet [71], § 3e
Cd	$5\,^1S_0-5\,^3P_1$	3261	$2\cdot5\times10^{-6*}$	—	Koenig and Ellett [30], § 3e
,,	,,	,,	$2\cdot5\times10^{-6*}$	0·0019	Kuhn [32], § 5a
,,	,,	,,	$\sim2\times10^{-6}$	—	Soleillet, chap. v
,,	,,	,,	$2\cdot3\times10^{-6*}$	—	Ellett, chap. v
,,	$5\,^1S_0-5\,^1P_1$	2288	$1\cdot98\times10^{-9*}$	1·20	Kuhn [32], § 5a
,,	,,	,,	$1\cdot99\times10^{-9*}$	—	Zemansky [90], § 4e
,,	,,	,,	$\sim10^{-9}$	—	Soleillet, chap. v
Tl	$6\,^2P_{3/2}-7\,^2S_{1/2}$	5350	(τ of $7\,^2S_{1/2}$ state is	0·076*	Prokofjew and So-lowjew [57], § 6c
,,	$6\,^2P_{1/2}-7\,^2S_{1/2}$	3776	$1\cdot4\times10^{-8}$)	0·08*	Kuhn [32], § 5a
,,	$6\,^2P_{1/2}-6\,^2D_{3/2}$	2768	—	0·20*	Kuhn [32], § 5a

Atom	Series notation of resonance line	Wave-length	τ in secs.	f-value	Author, reference and method
Hg	$6\,^1S_0-6\,^3P_1$	2537	$\sim1\times10^{-7}$	—	Webb and Messenger [79], § 3c
,,	,,	,,	$1\cdot08\times10^{-7*}$	—	Garrett [12], § 3c
,,	,,	,,	$0\cdot98\times10^{-7}$	—	Wien [84], § 3f
,,	,,	,,	$1\cdot0\times10^{-7}$	—	Füchtbauer, Joos and Dinke-lacker, as calculated by Tol-man [11, 74], § 4a
,,	,,	,,	$1\cdot08\times10^{-7*}$	0·0278	Kopfermann and Tietze, as calculated by Zehden and Zemansky [31, 87], § 4f
,,	,,	,,	$1\cdot14\times10^{-7*}$	0·0255	Ladenburg and Wolfsohn [41], § 6c
,,	,,	,,	$1\cdot13\times10^{-7}$	—	von Keussler, Chap. v
,,	,,	,,	$1\cdot08\times10^{-7*}$	—	Olson, recalculated by Mitchell, Chap. v
,,	,,	,,	$\sim10^{-7}$	—	Breit and Ellett, Chap. v
,,	,,	,,	$\sim10^{-7}$	—	Fermi and Rasetti, Chap. v
Hg	$6\,^1S_0-6\,^1P_1$	1849	$0\cdot3\times10^{-9}$	—	Garrett [12], § 4f
,,	,,	,,	$1\cdot6\times10^{-9}$	0·96	Ladenburg and Wolfsohn [43], § 6b
,,	,,	,,	$1\cdot30\times10^{-9*}$	1·19	Wolfsohn [85a], § 6c

Figure 17: The lower table shows a list of measurements of the lifetimes of the dominant excited states of mercury. For our information, several other elements have been used in a Hanle-effect experiment, which are shown in the upper table.

3 Apparatus and Procedure

3.1 Overview of apparatus

The goal in this experiment is to observe the intensity of resonantly scattered radiation (light) as a function of applied magnetic field, and from an analysis of intensity vs. applied field, derive the lifetime of the excited state responsible for the scattering.
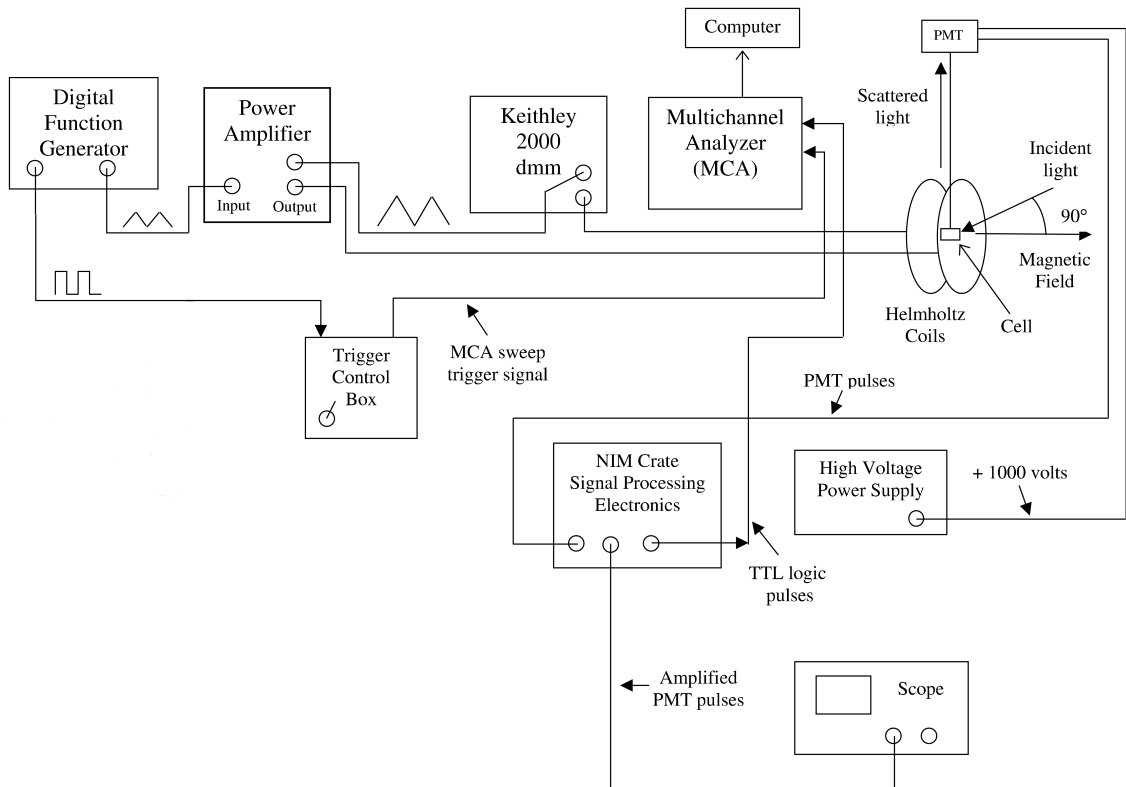

Figure 18: Schematic of Hanle effect apparatus.

The direction of the incident light, the direction in which the scattered light is observed, and the direction of the magnetic field are all mutually orthogonal. The geometry of our apparatus corresponds to Case (4) in section 1 of this write-up. The mercury cell in which the resonant scattering takes place is located at the center of a set of Helmholtz coils. This coil pair generates the applied field, which, having triangular waveform, varies linearly in time.

A second coil, sharing a common center with the Helmholtz pair, is used to cancel out the earth's field. When the axis of this coil is aligned parallel to the earth's field, a current of approximately 200 mA through this coil, known as a bucking coil, will cancel out the earth's field at the location of the mercury cell. A horizontal compass and vertical tiltmeter are available in the lab to check that the table holding the apparatus and the bucking coil are oriented such that the bucking coil axis is parallel the earth's field.

The applied magnetic field is swept symmetrically about zero with period slightly greater than 20

18

seconds. The triangular waveform is generated by a function generator and buffered by a power amplifier to provide the necessary current for the Helmholtz coils.

The scattered light is detected by a photomultiplier tube (PMT). Each incident photon that frees an electron from the photocathode of the PMT results in a pulse on the PMT output. This pulse is conditioned by several electronic circuits and turned into a TTL logic pulse. The logic pulse is counted by an instrument known as a multichannel analyzer (MCA). The number of pulses counted per unit time by the MCA is proportional to the light intensity.

The MCA is operated in the multichannel scaler (MCS) mode. In this mode, the MCA displays the total number of counted pulses (counts) on the vertical axis vs. time on the horizontal axis. The MCA is operated in this mode for the Hanle experiment, as time on the horizontal axis can be correlated with applied magnetic field, the parameter of interest in deriving the excited state lifetime. In the MCS mode, the MCA stops, or dwells, at each channel for a preset length of time (called the dwell time—same for all channels), increments the number of counts in that channel by the number of counts received during that time, and then moves on to the next channel. The time sweep starts at channel 0, finishes at channel 1023, and is initiated when a trigger signal is received by the MCA. This trigger signal is generated at the negative extreme of the triangular waveform.

To calibrate the horizontal axis of the MCA in terms of current, one needs to know the dwell time of the MCA, the period of the triangular waveform, and the maximum positive and maximum negative (termed maximum and minimum, respectively, for the remainder of the write-up) current through the coils. The waveform period is accurately controlled by the digital function generator maximum and minimum current values can be captured by the Keithley 2000 dmm.

3.2   Procedure

A schematic of the electronics is shown in Fig. 18. Turn on all electronics *except the Exact 170 power amplifier*: turn on the NIM bin, Wavetek 29 digital function generator, Keithley 2000 DMM, oscilloscope, and small power supply located under the coils. The little supply provides current for the bucking coil. Check that this supply is set for approximately 200 mA.

Caution: *the mercury lamp emits ultraviolet light which can cause damage to your eyes.* The UV is blocked by the glass disk, but it is nonetheless prudent to avoid looking directly at the lamp even through the protective glass. The optics in this experiment (lamp envelope, polarizer, mercury cell, optical filter, PMT envelope) are all fabricated of quartz, which transmits UV light (light of wavelength less than 400 nm). The glass disk which shields the lamp from direct view is made of Pyrex which transmits visible light but blocks UV.

Turn on the mercury lamp and the power supply for the lamp cooling fan. The latter two devices are on the cart holding the coils and apparatus.

Locate the high voltage power supply in the NIM bin; check that the voltage-adjust knobs are set to 0 volts. Flip the switch on the upper channel (A), and slowly turn the knob so that the outer scale shows a "1" in the little window and the dial is exactly at ".00". This gives 1000 volts. The current meter should be 2/3 of maximum. This power supply provides the bias for the PMT.

Caution: the UV polarizer is a very expensive—it would cost over \$700 to replace. Please be careful to avoid any contact with the surface of the polarizer when working nearby.

Check that the polarizer is set to the angle that maximizes the transmission of horizontally polarized light, i.e., light polarized parallel to the magnetic field. This angle is noted on the polarizer holder.

The angle reference mark is at the top of the dial. If the polarizer is not at this angle, carefully rotate it as necessary using the small pegs on the front of the polarizer holder.

You should now be able to see the (amplified) PMT output pulses on the oscilloscope. They are of negative polarity, approximately 10 nanoseconds in duration and 50 to 100 millivolts in amplitude. Some adjustment of the scope triggering may be necessary to get a display of the pulses.

Once you have a display, block the light path by carefully slipping an index card between the polarizer and the long aluminum tube and observe that the pulses disappear from the scope and reappear when you remove the card. Observe the intensity (brightness) of the scope display as you rotate the polarizer 90°. Note whether the intensity of the scope display increases or decreases. Explain your observations. Leave the polarizer in the orientation which maximizes the transmission of *vertically* polarized light.

Turn the digital function generator (Wavetek 29) on. The period of the triangular waveform and the auxiliary trigger output needs to be set so as to be in co-ordination with the MCA time sweep (remember that the sweep is triggered at the negative extreme of the triangular waveform). The dwell time per channel on the MCA will be set to 20 milliseconds, so the total sweep time for all 1024 channels will be 20.48 seconds. You must adjust the frequency of the function generator so that its period exceeds 20.48 seconds by a sufficient amount; 21 seconds is fine. (What would happen to the data collection if the function generator period is just under 20.48 seconds?)

To adjust the frequency and waveform of the digital signal generator, follow these steps:

1. Set the FUNCTION to TRIANGLE.

2. Push the FREQ/PER button, and then use the FIELD and DIGIT buttons to position the cursor on the numerical part of the period reading.

3. use the keypad to enter '2', '1', and then 'mHz s %' to set the period to 21 seconds.

Then set the trigger pulse phase as follows, in order to make the trigger edge line up with the negative extreme of the triangle wave:

1. Push the EDIT and then the TRIG buttons.

2. Use the FIELD buttons to move the cursor to the phase field.

3. Push '9', '0', '+/−' and ENTER to set the phase of the AUX OUT signal to −90°.

A suitable range of magnetic field is ± several gauss. Given the current to magnetic field conversion factor of 14.3 gauss/ampere, this implies a current range of $\approx \pm 200$ mA (400 mA peak-to-peak). With a knowledge of the coil resistance, amplifier input and output impedance and amplifier gain, and function generator output impedance and maximum amplitude, you can estimate the amplitude setting of the function generator necessary to produce a current of 200 mA.

- The Helmholtz coil resistance is approximately 10 ohms.

- The Exact model 170 amplifier has two possible voltage gains: $\times 2$ and $\times 10$. The output impedance of the amp is 50Ω using the front panel BNC connector and 600Ω using the banana plug connectors. The input impedance is 600Ω.

- The maximum output from the function generator is 5 volts into a 50Ω load. The output impedance is 50Ω.

Given these facts, draw a circuit diagram using Thévenin equivalents of the function generator, amplifier and coils so that you can work out what peak amplitude settings and gain needed to create 200 mA in the coils.

Then, using a procedure similar to the above for setting the frequency and auxiliary phase, set the amplitude of the function generator output to the desired value.

Turn the Exact 170 amplifier on, and check to make sure the correct gain setting is selected.

Finally, turn the OUTPUT of the Wavetek 29 function generator to ON. (If needed, you may use a second oscilloscope to look at the output of the function generator. One of the Tektronics digital scopes are best here, since the waveform period is so long.)

With the Keithly 2000 dmm on, set the meter to 'DC-I'. If all is working correctly, you should see the readings change slowly from about -0.20 A to $+0.20$ A (give or take). The Keithley 2000 dmm is used to capture the maximum and minimum (most negative) current values, which you will need in order to find the range of magnetic field applied by the Helmholtz coils. If you do not see that the current readings are close to what was expected, try adjusting the amplitude settings a bit. If they are way off what you expected, double check your calculations and ask for help if needed.

You will need use the Keithley meter to record the maximum and minimum current sent to the Helmholtz coils. To do this, a set of readings is stored in the dmm buffer, and after the storage cycle is complete, the maximum and minimum values can be read out. Instructions for using the buffer are as follows:

Keithley 2000 settings:

Current range:	1 ampere; **important:** if it is set to autorange, the dmm will change ranges as the current is being swept and introduce a discontinuity in the coil current;
Filter:	OFF;
Rate:	MED (medium).

With the reading rate set to medium and a waveform period of approximately 20 seconds, 1024 readings are sufficient to always capture the maximum and minimum current values.

To acquire a set of readings:

1. Press the STORE key.

2. Use the ◄, ►, ▲, ▼ keys to set the number of readings to 1024 (◄ and ► keys select the digit to be set; ▲ and ▼ keys set the value of the selected digit); you need set this number only once.

3. Press ENTER to initiate the acquisition of the readings. The ∗ annunciator on the front panel will be on while the readings are being taken and stored.

To view the maximum and minimum readings:

1. Press the RECALL key; the BUFFER annunciator will come on to indicate that stored readings are being displayed.

2. Press the ▼ key three times to bring the buffer to the minimum reading location, and then press the ► key to display the minimum. To display the maximum reading, press the ◄

key, then the ▼ key and then the ▶ key. To return to the regular display, push the EXIT key. Several pages from the Keithley 2000 dmm manual are available in the lab for further information on these operations.

3. To take another set of readings, press the STORE and then ENTER keys.

Take several sets of readings to make sure that you are capturing the maximum and minimum values, or something very close to them. The values for the maximum and minimum should not vary by more than $\approx \pm 1$ mA from one set to the next.

In the MCS mode, the MCA will execute 9999 sweeps and then stop. At the top of the screen is a sweep counter, which counts down the number of sweeps starting at 9999. To get reasonable data, it is not necessary to sweep this many times (indeed, 9999 sweeps would take more than two days at the typical sweep rate for this experiment). You can judge from the appearance of the data on the screen as to when the scatter in the data has been reduced to a reasonable level and terminate data collection at that point in time. In most cases, 30–40 minutes of data accumulation should be more than sufficient for the data used to derive the excited state lifetime.

To check out the MCA settings, press the SET UP key and then the MCS key. Step through the parameters by pressing the CONT key.

The parameters should be set to:

ADD	(adds counts instead of subtracting them)
ALL	(means data goes into all 1024 channels)
SWEEPS	(you can preset the desired number of sweeps here if you like)
T/CH = dwell time	(should be set to 20 milliseconds)

To exit the SET UP routine press the TERM button.

To clear the data in memory, press the following buttons in sequence: 0, GOES INTO, ALL.

To initiate data acquisition, press the RUN and then MCS buttons. For the sweep trigger signal to reach the MCA, the Trigger Enable/Disable switch on the MCS Trigger Control box must be in the Trigger Enable position. Check that the separate 5 volt power supply for this box is turned on. To interrupt data collection at any time, move the switch to the Trigger Disable position. The sweep in progress will finish and the MCA will not resume data collection until the switch is returned to the Trigger Enable position.

To end data collection first flip the Trigger Enable/Disable switch to Disable, and let the data sweep finish. Then press the TERM button on the MCA. (Note, When you press the RUN and MCS buttons to start data collection again, the sweep counter will reset to 9999 or the value to which you set it in the SET UP procedure.) Stopping data collection with the Trigger Enable/Disable first keeps the MCA from stopping in the middle of a run. (It als allows you to preserve the sweep count when you resume data collection, unlike stopping and starting data collection using the MCA controls.)

To transfer data to the computer, turn on the computer and login according to the TA or manager's instructions (it may already be running). Open the LabVIEW application "Norland Interface" which should be available on the desktop. When the application is loaded, start the program by clicking on the "arrow" button at the top left corner.

When the program starts, it will show the most recent data set that was loaded from the MCA. To transfer your data to the computer:

1. Make sure that the READY annunciator is visible at the lower left corner of the MCA screen.

2. Click the green "Read data from MCA" button.

3. Press "RUN" followed by the softkey "I/O" on the MCA.

You will see the "I/O" indicator light up on the MCA—this indicates that data is being sent over the serial line to the computer. As soon as the I/O indicator goes out (about 15 seconds), you will see your data appear on the screen.

After your data has loaded, you can save it to a file, analyze the data with the peak-fitting routine, print the data and comments on the lab printer, and load old data sets for examination and analysis. Instructions for the program are available from the "SHOW INSTRUCTIONS" button. You should make sure to save your data to a floppy disk or other off-computer storage device (i.e., email, memory stick, etc.); we cannot guarantee that your data will remain on the computer.

The data will show two dips in the intensity corresponding to two passages through the zero field condition. The spacing between the centers of the two dips should correspond to $\frac{1}{2}$ the period of the function generator, provided that the magnetic field sweep is symmetric about zero.

To determine the lifetime of the excited state it is necessary to measure the half width at half maximum of the intensity dip, as shown in Fig. 11. You can use the peak-fitting dialog box to fit the (inverted) peaks to a Lorentzian line shape. One of the fitting parameters controls the peak width, and can be used to deduce the half width at half maximum. Further instructions on how to operate this part of the program are under the "SHOW INSTRUCTIONS" button.

You will measure the half width at half maximum in channels, which can be converted to magnetic field to derive a value for $\Delta B_{1/2}$. To convert to magnetic field, you will need to know

- the dwell time per channel,

- the period of the function generator, which should be twice the time separation of the centers of the dips.

- the maximum and minimum values of the current,

- the factor by which to convert current in the Helmholtz coils to magnetic field produced by the coils. This factor is

$$14.3 \text{ gauss/ampere.}$$

Once you have determined $\Delta B_{1/2}$, the mean lifetime τ can be derived using Eq. 4.

3.3   Changing the polarizer orientation

Having acquired data with the polarizer in the orientation corresponding to Case (4), it is interesting to rotate it 90° and observe the effect on the measured light intensity. Now, rotate the polarizer to the orientation which maximizes the transmission of horizontally polarized light. Clear the MCA memory and acquire data (a few tens of sweeps should suffice) with the polarizer in the new orientation. Explain the appearance of the data, and associate this configuration of the experiment with the appropriate Case from Section I.

23

3.4 The importance of the bucking coil

Finally, in order to appreciate the need to cancel out the earth's field with the bucking coil, it is instructive to take short data runs with and without the bucking coil current on. Return the polarizer to the position maximizing the transmission of vertically polarized light. With the bucking coil current still on, clear the memory and set up the MCA to acquire data over 20 sweeps. Save this data on the computer. Now turn off the current to the bucking coil. Clear the memory and again acquire data over 20 sweeps. Compare the results for bucking coil current on and off and explain the qualitative differences.

3.5 Shut down

Turn off all the electronics, except the lamp cooling fan (don't forget the bucking coil power supply). After the lamp has cooled a minute or two, turn off the cooling fan. Place the cover over the polarizer.

Prepared by R. Van Dyck, J. Stoltenberg and D. Pengra
`hanle-effect.tex` -- Updated 8 May 2023